Non-Destructive Damage Identification in Hydrothermally Aged Unidirectional Glass Fiber Tapes Using Acoustic Emission and Unsupervised Learning

J. Palacios Moreno[1] and P. Mertiny[1*]

[1] Department of Mechanical Engineering, University of Alberta, Edmonton, Canada

* *Corresponding author (pmertiny@ualberta.ca)*

Keywords: *glass-fiber thermoplastic tapes; non-destructive technique; acoustic emission, hydrothermal aging; unsupervised learning*

1. Abstract

Unidirectional glass fiber-reinforced thermoplastic (UGFT) composite tapes are increasingly viewed as high-performance, recyclable structural materials for demanding industrial applications such as composite pressure pipes and other lightweight load-bearing components. Despite their attractive stiffness-to-weight ratio and manufacturing advantages, their long-term durability in hot, wet service conditions remains a major concern. Hydrothermal exposure can accelerate moisture ingress, promote matrix softening, degrade fiber-matrix bonding, and ultimately reduce the mechanical integrity required for safety-critical systems. In this context, the present study highlights a non-destructive approach to evaluate aging behavior in polyethylene-based UGFT tapes under controlled hydrothermal conditions. Specimens were conditioned at 95°C in a distilled-water environment for exposure durations up to four weeks. A complementary measurement technique was systematically integrated to quantify degradation and track damage evolution. Thus, tensile testing was performed to measure strength retention after conditioning, with a greater than 25% reduction in tensile strength defined as a practical threshold indicating significant deterioration. A central feature of this approach was acoustic emission (AE) monitoring as a non-destructive tool to capture transient waveforms generated during mechanical loading. AE waveform descriptors, such as amplitude, rise time, energy, and frequency content, were used as measurable signatures of internal damage events, including matrix cracking, interfacial debonding, and fiber breakage. Given the large volume and complexity of AE data, principal component analysis (PCA) was applied to reduce dimensionality, followed by k-means clustering to group signals into distinct damage categories. Finally, optical microscopy provided microstructural verification of damage classifications and supported the physical interpretation of AE-based results. This integrated framework offers a pathway to monitor, identify, and quantify damage development in hydrothermally aged UGFT structures.

2. Introduction

Unidirectional glass fiber-reinforced thermoplastic (UGFT) composite tapes offer high toughness and damage tolerance, making them promising alternatives to thermoset composites for structural applications [1]. However, their wider use is limited by processing and durability challenges [2]. Compared with thermosets, thermoplastics require higher processing temperatures and have higher melt viscosity, which can hinder consolidation. During service, matrices such as polyethylene (PE) may also soften under elevated temperatures, while thermally induced stresses can weaken the fiber-matrix interface and reduce load transfer. These issues are critical for UGFT tapes used as reinforcements in thermoplastic composite pressure pipes and other lightweight load-bearing components exposed to long-term hydrothermal conditions. Previous studies show that moisture uptake and hydrothermal aging can reduce glass transition temperature and mechanical properties through moisture retention, plasticization, and interfacial degradation [3]. In continuous-fiber composites, hydrothermal exposure has caused early strength loss, weakened fiber/matrix bonding, increased fiber pull-out, and reductions in tensile, compressive, and flexural strength [4]. Therefore, durability assessment must link mechanical property loss with internal damage evolution. Acoustic emission (AE) provides a useful non-destructive method to monitor damage progression in aged composites. AE descriptors, combined with clustering methods, can identify changes in damage activity caused by hydrothermal exposure and can be supported by microscopic or Scanning Electron Microscope analyses [5]. Thus, PCA and k-means clustering have been used to distinguish matrix cracking, interfacial debonding, delamination, and fiber breakage [5,6,7]. This study develops a metrology-driven framework to evaluate UGFT tensile performance after immersion in distilled water (DW) at 95°C for up to four weeks, representing pipeline-relevant service conditions and other engineering applications. Strength losses above 25% are considered structurally significant. AE monitoring is performed during fiber-direction tensile loading of pristine and aged specimens to track matrix cracking, debonding, and fiber breakage. Signal-derived AE descriptors are used for noise-tolerant analysis, followed by principal component analysis (PCA) [8] for feature reduction and k-means clustering for damage-mode classification [7].

3. Materials and methods

3.1. Materials

Commercial glass fiber-reinforced polyethylene (GF-PE) tapes were used in this study. This material was selected because its thin cross-section enables accelerated hydrothermal aging: reduced thickness promotes faster moisture saturation, allowing water-uptake behavior and property changes to be captured over short immersion times. The tested tape was grade UD-002 (Qingdao Trusmax New Material Co. Ltd., Shandong, China) with nominal dimensions of 0.3 mm thickness and 49 mm width, providing good dimensional consistency and reproducible exposure conditions. Fiber weight fraction was verified by ash content testing following established procedures [9], confirming agreement with the supplier specification of 60 ± 5%. In addition to tape testing, glass fiber specimens were also tested to better isolate and interpret fiber-breakage signatures. Table 1 summarizes the test types, specimen counts and dimensions, and the expected damage mechanisms.

Table 1. Experimental conditions and corresponding AE-identified damage mechanisms.

Material	Number of Samples	Dimensions	Expected Damage Mechanisms
GP-PE tape tensile test	5	Length = 250 mm Width = 49 mm Thickness = 0.5 mm	Matrix cracking and matrix/fiber debonding
Fiber tensile test	10	N/A	Fiber breakage

3.2. Acoustic emission setup and procedure

Figure 1 illustrates the experimental setup used to study damage mechanisms in GF-PE tapes and glass fiber specimens, following [6]. AE data were collected during mechanical testing using a Micro-SHM system (Physical Acoustics, West Windsor Township, NJ, USA) with AEWin software (V1.21), as shown in Figure 1(a), 1(b) and 1(c). Signals were recorded with a PK15I medium-frequency resonant piezoelectric sensor incorporating a 26-dB low-noise preamplifier. To limit background noise and ensure consistency with prior studies [5-7,10], a 45-dB threshold was applied. Post-processing was conducted in the selected computational environment using an unsupervised learning workflow to classify AE waveforms and distinguish damage modes. Two channels (Ch1, Ch2) were used to improve spatial resolution and event localization, with hit detection times (HDTs) of 50 µs (Ch1) and 100 µs (Ch2). The acquisition settings also included a peak detection time (PDT) of 50 µs and a hit lock time (HLT) of 100 µs to reduce overlap and improve event discrimination. These timing parameters were chosen based on prior works on polymer composite systems with similar AE behavior [5-7,10], supporting reliable identification of matrix cracking, interfacial debonding, and fiber breakage, as shown Figure 1(d).

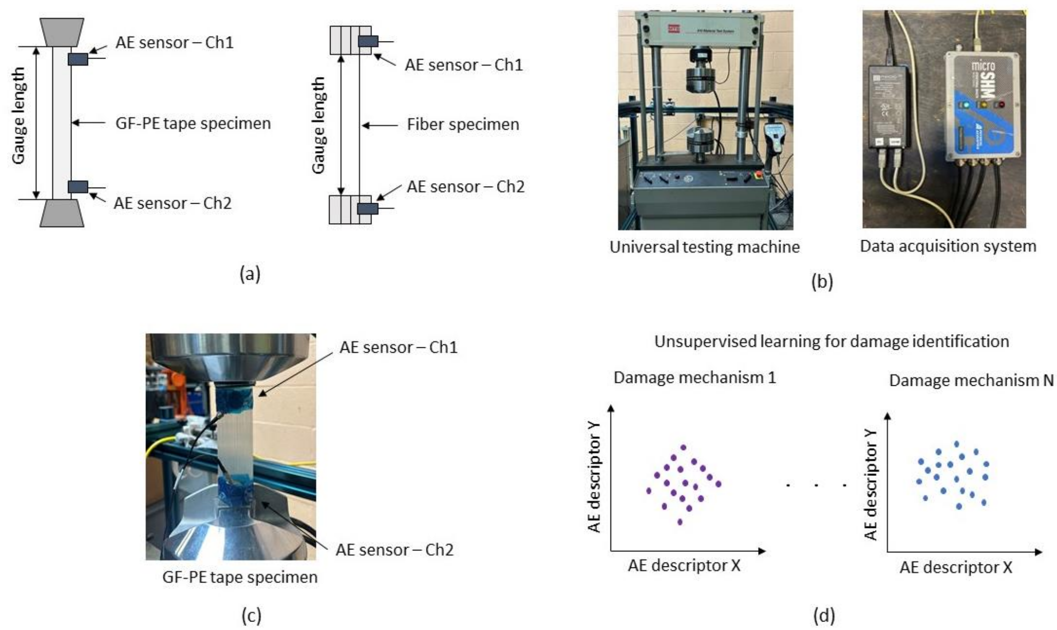

Figure 1. (a) Schematics of tensile testing of GF-PE specimen and test setup for fiber-breaking force measurement; (b) photographs of universal testing machine and AE data acquisition system; (c) photograph of tensile testing of GF-PE specimen; and (d) schematic of unsupervised learning methods for damage identification and classification.

3.3. Aging conditions and mechanical testing

Hydrothermal aging was conducted under controlled but aggressive conditions to simulate service-relevant exposure. Tape specimens were immersed in DW and conditioned at 95°C to accelerate degradation without exceeding temperatures that could trigger non-representative failure. Aging periods of 1 and 4 weeks were selected as practical accelerated intervals that capture measurable property changes within laboratory timescales. A >25% reduction in tensile strength was defined as structurally significant for comparing degradation severity across conditions. Aging was performed in sealed glass jars placed in a temperature-controlled oven to ensure stable exposure while minimizing contamination, evaporation, and concentration changes. Glass fibers were not aged because the study focused on degradation mechanisms in the GF-PE tape system. GF-PE tapes were tensile tested in air at room temperature (RT) using an MTS 810 universal testing machine (Eden Prairie, MN, USA) with a 100 kN load cell (Figure 1(c)). Tests followed ASTM D3039-17 [11] with a 150 mm gauge length and 5.0 mm/min crosshead speed. For each aging condition, five specimens were tested. Grip effects were reduced using sandpaper, protective tabs, and aluminum tape. To provide an independent reference for fiber strength, single-fiber tensile tests were performed at RT using Capstan grips according to ASTM D2256M-21 [12]. Tests used an approximate 250 mm gauge length and 250 mm/min displacement rate. At least ten fiber strands were tested, and fiber strength was taken as the maximum load before the sudden drop at failure.

3.4 Principal component analysis

PCA is a statistical technique used to simplify multidimensional datasets by converting a set of correlated variables into a smaller number of uncorrelated variables called principal components [8]. PCA identifies the directions in the data that contain the most variability: the first component captures the maximum variance, and each subsequent component explains the next highest variance while remaining orthogonal to the previous ones. The transformed values (scores) represent each observation projected onto these new axes, reducing redundancy and emphasizing the dominant patterns in the dataset [8]. PCA is typically implemented using matrix decomposition methods (e.g., SVD), where the variance explained by each component is used to decide how many components to retain for further analysis.

3.5 K-means algorithm

The K-means algorithm [7] is an unsupervised clustering method that partitions a dataset into a predefined number of clusters by minimizing within-cluster variability. It starts by selecting initial cluster centers (centroids), then assigns each data point to the nearest centroid using Euclidean distance. The centroids are updated as the mean of the assigned points, and the assignment–update steps are repeated until the clusters stabilize (i.e., assignments or centroid positions change negligibly).

4. Results

4.1. Principal component analysis for pristine and aged samples

AE data from pristine and aged samples were arranged in a matrix [X] with m AE hits and n = 14 descriptors: rise time (RISE), counts (COUNT), energy (ENER), duration (DURATION), amplitude (AMP), average frequency (A-FRQ), root mean square (RMS), counts to peak (PCNTS), reverberation frequency (R-FRQ), initiation frequency (I-FRQ), signal strength (SIG-STRENGTH), absolute energy (ABS-ENERGY), centroid frequency (C-FRQ), and peak frequency (P-FRQ). Following [6], strongly skewed descriptors, especially duration and energy, were log-transformed, and all variables were normalized before PCA. PCA projected the data onto PC1-PC2. Descriptor selection was based on eigenvector loadings and two criteria [6,7]: (i) removal should not cause significant information loss, and (ii) selected descriptors should be distinct in direction/magnitude. Figure 2(a) shows the PC1-PC2 projection for pristine GF-PE (baseline: as received) and samples aged at 95 °C in DW. Since both channels showed similar behavior, Channel 1 was used. For pristine samples, peak frequency, amplitude, rise time, energy, and duration were identified as the most relevant descriptors. PC1 and PC2 explained 46.77% and 27.43% of the variance, respectively, giving 74.2% total variance. Higher PCs mainly added noise or redundancy; therefore, clustering used PC1-PC2 only. For 1- and 4-week aged samples (Figure 2(b) and 2(c)), the same descriptors remained dominant. PC1-PC2 explained 65.97% of the variance after 1 week and 71.84% after 4 weeks. The Davies-Bouldin (DB) index indicated three optimal k-means clusters, corresponding to the main GF-PE damage mechanisms: matrix cracking, fiber/matrix debonding, and fiber breakage.

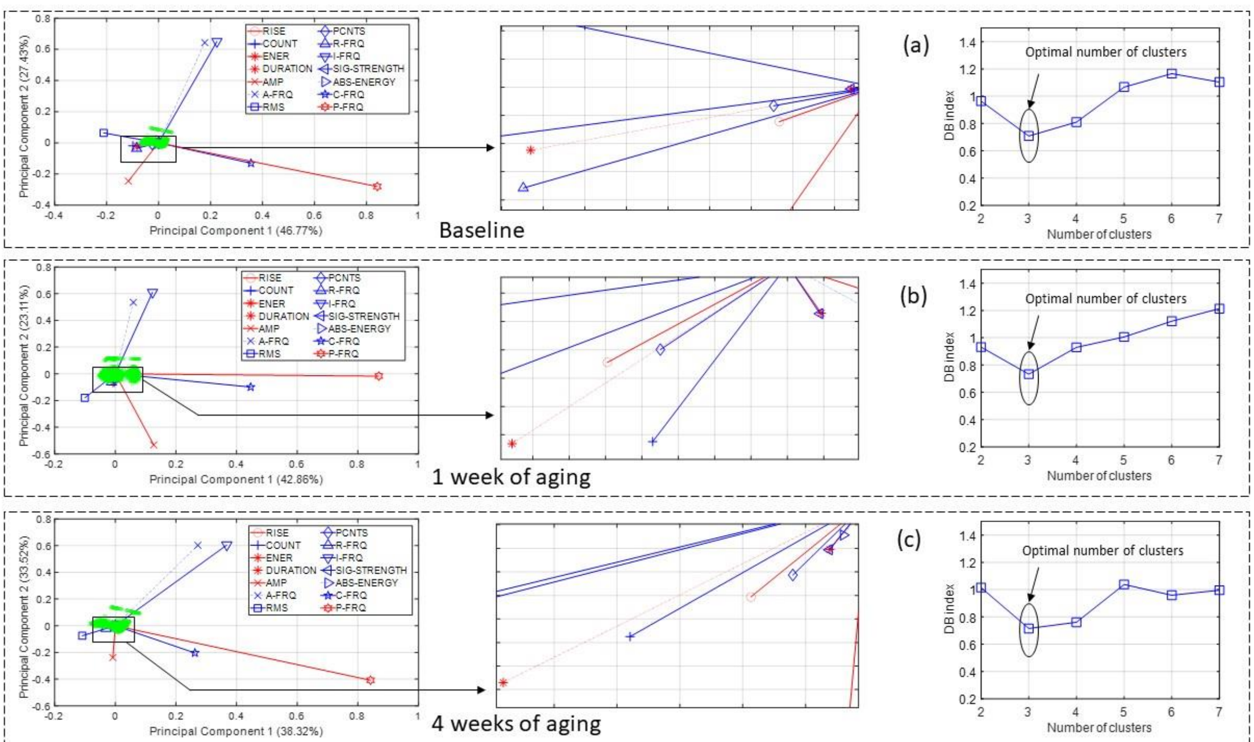

Figure 2. PCA projection of Ch1 AE descriptors onto PC1–PC2 for GF-PP tapes, with DB index used to select clusters for (a) baseline, (b) 1-week aging, and (c) 4-week aging.

4.2. Acoustic emission measurements from individual experiments

After selecting the optimal number of clusters, each cluster was assigned to its corresponding damage mechanism: fiber breakage (damage mechanism #1), matrix cracking (damage mechanism

#2), or fiber/matrix debonding (damage mechanism #3). Figure 3 shows the AE amplitude-peak frequency evolution for fiber specimens and GF-PE tapes before and after hydrothermal aging, highlighting changes in dominant damage mechanisms. Table 2 confirms that the identified frequency bands agree with literature values.

Table 2. Damage mechanisms of GF-PP tape specimens based on AE peak frequency bands in kHz and comparison with frequency bands available in the technical literature.

Reference	Fiber-Matrix Type	Matrix cracking	Matrix/Fiber debonding	Fiber breakage
Present work		85-210	230-340	350-500
[13]	GF-Polypropylene	80-120	240-350	380-570
[14]	GF-Polyester	10-150	150-250	350-500

Figure 3(a) shows AE signals from fiber specimens within 350-500 kHz and 45-84 dB. Since no matrix was present, these signals are attributed to fiber-related damage. The small cluster at 350-378 kHz is assigned to friction between broken and load-bearing fibers, while the stronger cluster at 400-500 kHz is linked to fiber breakage [6]. Thus, 350-500 kHz is defined as fiber-dominated damage mechanism #1, consistent with [13,14], in which the ranges are 380-570 kHz and 350-500 kHz, respectively. For the pristine GF-PE tape, Figure 5(b) shows three AE frequency bands. The 85-210 kHz range is associated with matrix cracking, defined as damage mechanism #2, based on frequency bands described for this damage mode in [13,14] ranging between 80 and 120 kHz and 10 and 150 kHz, respectively. The 230-340 kHz range corresponds to matrix/fiber debonding, defined as damage mechanism #3, based on the frequency band in [13] for this damage mechanism ranging between 240-350 kHz. Finally, the 350-500 kHz range represents fiber-related damage, as confirmed by the fiber specimens. After one week of hydrothermal aging, Figure 5(c) shows decreased AE activity, especially in the intermediate-frequency region. This suggests greater early interface weakening due to moisture absorption and polymer plasticization. The fiber-related region remains present but becomes less distinct. After four weeks, Figure 5(d) shows the 230-340 kHz matrix/fiber debonding and 350-500 kHz fiber-breakage regions becoming less populated in comparison with the pristine samples. This suggests reduced load transfer from the degraded matrix to the fibers. Therefore, hydrothermal aging might shift the damage response from combined matrix-interface-fiber damage toward matrix- and interface-controlled degradation. In terms of amplitude values, the range of 45-90 dB observed during the mechanical loading reflects the more heterogeneous and energetic nature of damage accumulation for all the conditions. Amplitude is commonly used as an AE descriptor; however, comparing amplitude trends across studies is challenging because AE responses depend on the testing setup and material system. In this study, the amplitude ranges of different damage events overlap, making it difficult to distinguish damage mechanisms using amplitude or peak frequency alone. Therefore, single AE descriptors are not sufficient for reliable damage identification in GF-PE tape specimens. This limitation supports the use of multivariable AE analysis. Accordingly, the next subsection applies k-means clustering to PCA-derived AE descriptors to obtain clearer groupings associated with distinct damage mechanisms.

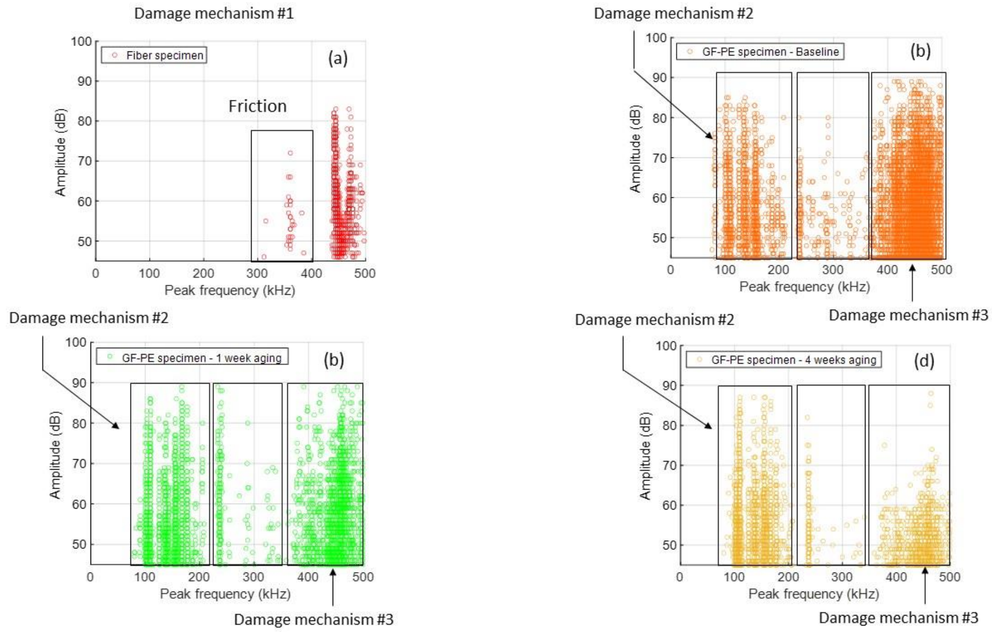

Figure 3. AE amplitude-peak frequency plots from: (a) fiber tensile tests, (b) baseline GF-PE tape, (c) GF-PE tape after 1-week aging, and (d) GF-PE tape after 4-week aging.

4.3. K-means clustering and mechanical performance analysis

This subsection examines the remaining PCA-selected AE descriptors and their relationship with the mechanical performance of unaged and aged GF-PE tape specimens. Five descriptors: rise time, amplitude, peak frequency, energy, and duration, were used as inputs for k-means clustering. The AE hits were grouped into three clusters and assigned to fiber breakage, matrix cracking, and matrix/fiber debonding. The results in Figure 4 shows the effect of hydrothermal aging at 95°C on the mechanical integrity, damage evolution, and failure behavior of GF-PE tapes. Strength retention in Figure 4(a) decreased to 79.21 ± 3.8% after 1 week and 51.03 ± 3.3% after 4 weeks, exceeding the 25% degradation threshold. This suggests a severe reduction in load-bearing capacity due to moisture-induced matrix plasticization and interfacial weakening. In Figure 4(b), baseline specimens show fiber-dominated failure, with rupture at 357.43 MPa after 54.29 s. Fiber breakage is the dominant AE damage mode, followed by matrix cracking and matrix/fiber debonding, consistent with the high fiber volume fraction of 60 ± 5% [5]. After 1 week, Figure 4(c) shows a reduced peak stress of 313.49 MPa at 44.93 s. After 4 weeks, Figure 4(d) shows further degradation, with peak stress decreasing to 221.83 MPa at 26.8 s and a more unstable stress response. AE hit counts and energy distributions confirm that fiber breakage dominates all conditions. In Figure 4(b), fiber breakage accounts for 66.17% of hits, followed by matrix cracking at 28.33% and matrix/fiber debonding at 5%. However, the energy distribution is more balanced, with contributions of 49.45%, 25.97%, and 24.58%, respectively. In Figure 4(c), fiber breakage increases to 83.36% of hits and 53.64% of energy, while matrix cracking and debonding decrease in hit count to 15.64% and 1%. In Figure 4(d), fiber breakage remains dominant, contributing 78.56% of hits and 74.04% of energy, while matrix cracking and debonding contribute 20.2% and 1.34% of hits, and 23.32% and 2.64% of energy, respectively. The combined changes in AE hit counts and energy might indicate that hydrothermal aging gradually degrades the matrix and interphase, reducing matrix support and promoting a transition toward brittle, fiber-dominated fracture in UGFT composites [5,6].

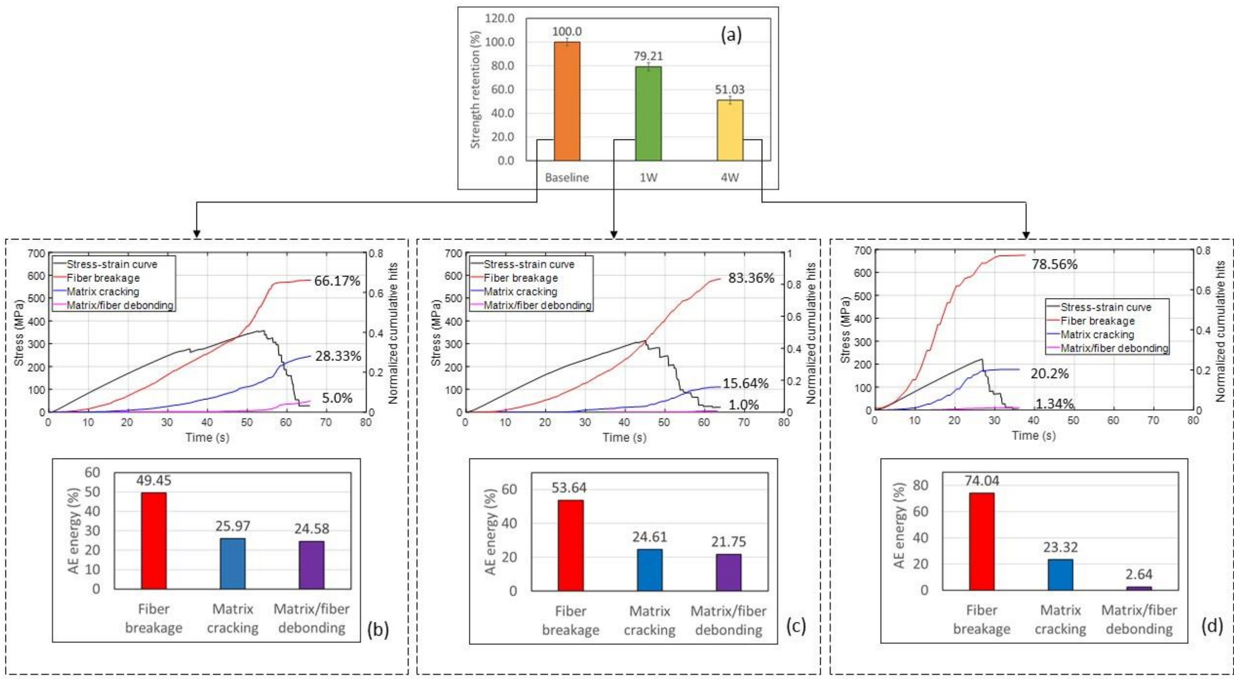

Figure 4. (a) Strength retention of GF-PE tapes after 1 and 4 weeks in DI water. Stress curves, normalized cumulative damage hits, and energy contribution for (b) baseline, (c) 1-week aged, and (d) 4-week aged specimens.

4.4. Cluster analysis using AE descriptors and microscopic observations

The remaining AE descriptors, rise time and duration, can be analyzed together with amplitude using the RA value. As described in [6,10], the RA value is an effective parameter for distinguishing tensile and shear events in composite materials during mechanical loading. It is calculated as the ratio between the rise time of an AE hit and its peak amplitude. Tensile-driven events, such as matrix cracking and fiber fracture, typically produce RA values below unity, whereas shear-related events, including matrix/fiber debonding, are generally associated with RA values above unity. In this study, RA was calculated using peak amplitude in dB, following the procedure in [10]. Figure 5 shows RA value versus duration for unaged and aged GF-PE tape specimens. In the baseline condition (Figure 5(a)), the three damage mechanisms are separated: fiber breakage at RA < 1 μs/dB with durations up to 500 μs, matrix cracking at RA = 0.1-0.5 μs/dB with durations up to 1800 μs, and matrix/fiber debonding at RA = 1-2 μs/dB with durations between 1200-4200 μs. After 1 and 4 weeks of aging (Figure 5(b) and 5(c)), all clusters shift to shorter durations, slightly lower RA values and less AE events, which may indicate early matrix plasticization and interface weakening. Thus, from the baseline condition to 4 weeks of aging, AE hits exhibit a 10-20% decrease in duration ranges and a 5-10% reduction in RA ranges, which may indicate hydrothermal degradation of the matrix, interface, and overall mechanical response of the GF-PE tape specimens.

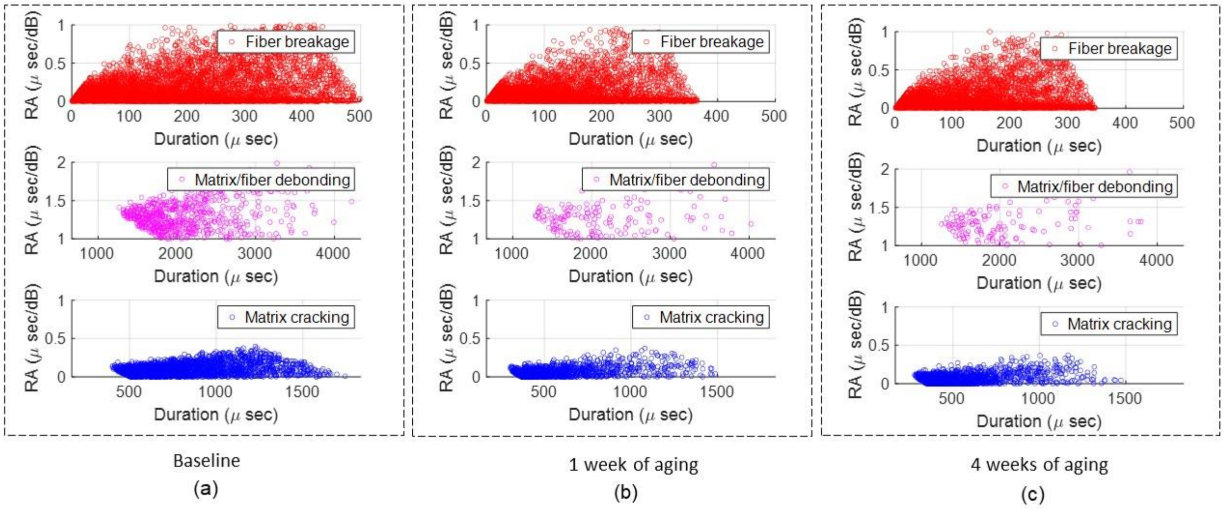

Figure 5. RA value versus AE duration for damage mechanisms in GF-PE tape specimens: (a) baseline, (b) 1-week aged, and (c) 4-week aged.

GF-PE tape specimens were also examined using an optical microscope after tensile testing. Figure 6(a) shows longitudinal deformation leading to catastrophic failure of a GF-PE tape specimen, as opposing tensile loads along the fiber axis induce both matrix- and fiber-dominated damage. Figures 6(b)-6(d) provide micro-mechanical evidence of these specific failure mechanisms in the case of baseline specimens: fiber breakage, matrix/fiber debonding and matrix cracking.

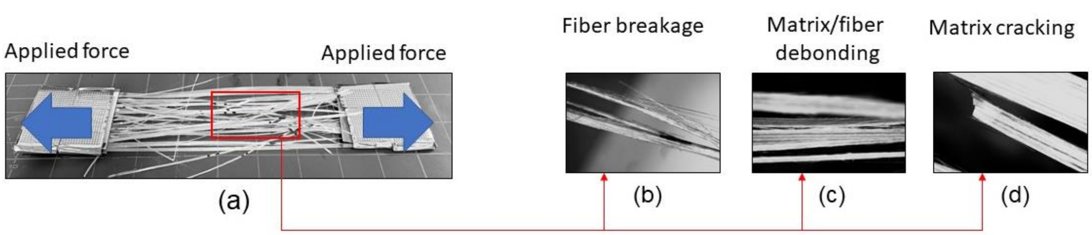

Figure 6. Microscopic images of a damaged GF-PE tape after tensile testing: (a) loading direction, (b) fiber breakage, (c) matrix cracking, and (d) fiber/matrix debonding.

5. Conclusion

This study developed an AE-machine learning framework to assess the tensile durability of GF-PE tapes aged in DW at 95 °C for up to 4 weeks, representing composite pressure pipe and lightweight load-bearing applications. After 4 weeks, strength decreased by 49.97%, exceeding the degradation threshold. Fiber breakage dominated AE hit counts (66.17-83.36%) and energy (49.45-74.04%), likely due to the high glass fiber content of 60 ± 5%. Matrix/fiber debonding was the least frequent mechanism, contributing 1-5% of hits and 2.64-24.58% of energy, while matrix cracking contributed 15.63-28.33% of hits and 23.32-25.97% of energy. Reductions in AE duration by 10-20% and RA values by 5-15% confirmed progressive matrix/interface degradation and reduced load transfer. Thus, AE combined with PCA and k-means clustering effectively identified damage modes and evaluated UGFT tape integrity. Future work should integrate supervised learning, such as neural networks, to improve automated damage classification.

6. References

[1] M. Nikforooz, J. Montesano, M. Golzar, M. M. Shokrieh. "Assessment of the thermomechanical performance of continuous glass fiber reinforced thermoplastic laminates". Polymer Testing. Vol. 67, pp 457-467, 2018.

[2] M. Nikforooz, J. Montesano, M. Golzar, M. M. Shokrieh. "Assessment of failure toughening mechanisms in continuous glass fiber thermoplastic laminates subjected to cyclic loading". Composites part B: Engineering, Vol. 161, pp 344-356, 2019.

[3] D. Gibhardt, A. Doblies, L. Meyer, B. Fiedler. "Effects of Hygrothermal Ageing on the Interphase, Fatigue, and Mechanical Properties of Glass Fibre Reinforced Epoxy". Fibers, Vol. 5, No. 7, pp 55, 2019.

[4] R. Zhu, X. Li, C. Wu, L. Du, X. Du, T. Tafsirojjaman. "Effect of Hydrothermal Environment on Mechanical Properties and Electrical Response Behavior of Continuous Carbon Fiber/Epoxy Composite Plates". Polymers, Vol.14, pp 4072, 2022.

[5] J. Chen, L. Lei, C. Ji, S. Yang, Z. Cheng, J. Fan, T. Yu. "Cluster analysis of acoustic emission signals for bending damage mechanism of flax fiber reinforced composites under hydrothermal aging". Composite Communications, Vol. 53, pp 102165, 2025.

[6] J. Palacios Moreno, P. Mertiny, "Acoustic Emission and Machine Learning Approaches for Assessing Mechanical Degradation in Aged Unidirectional Glass Fiber-Reinforced Thermoplastics". Metrology, Vol. 11, No. 1, pp 11 2026.

[7] W. Harizi, S. Chaki, G. Bourse, M. Ourak. "Damage mechanisms assessment of Glass Fiber-Reinforced Polymer (GFRP) composites using multivariable analysis methods applied to acoustic emission data". Composite Structures, Vol. 289, pp 115470, 2022.

[8] H. Abdi, L. J. Williams. "Principal component analysis". WIREs Computational Statistics, Vol. 2, No. 4, pp 433-459, 2010.

[9] ASTM D5630-22. "Standard Test Method for Ash Content in Plastics". ASTM International: West Conshohocken, PA, USA, 2023.

[10] H. Nazaripoor, H. Ashrafizadeh, R. Schultz, J. Runka, P. Mertiny. "Acoustic Emission Damage Detection during Three-Point Bend Testing of Short Glass Fiber Reinforced Composite Panels: Integrity Assessment". Journal of Composite Science, Vol. 6, No. 2, pp 48, 2022.

[11] ASTM D3039-17. "Standard Test Method for Tensile Properties of Polymer Matrix Composite Materials". ASTM International: West Conshohocken, PA, USA, 2017.

[12] ASTM D2343-17. "Standard Test Method for Tensile Properties of Glass Fiber Strands, Yarns, and Rovings Used in Reinforced Plastics". ASTM International: West Conshohocken, PA, USA, 2009.

[13] C. R. Ramirez-Jimenez, N. Papadakis, N. Reynolds, T. H. Gan, P. Purnell, M. Pharaoh. "Identification of failure modes in glass/polypropylene composites by means of the primary frequency content of the acoustic emission event". Composites Science and Technology, Vol. 64, pp 1819-1827, 2004.

[14] I. Amenabar, A. Mendikute, A. López-Arraiza, M. Lizaranzu, J. Aurrekoetxea. "Comparison and analysis of non-destructive testing techniques suitable for delamination inspection in wind turbine blades". Composites part B: Engineering, Vol. 42, pp 1298-1305, 2011.